USER'S GUIDE

Maynord Model User Guide

Tugboat-Induced Flows and Sediment Bed Erosion: Application of Maynord's Model in San Diego Bay

ESTCP Project ER-201031

AUGUST 2014

Pei-Fang Wang, Ph.D.
Blake Cole
Ripan Barua
Space and Naval Warfare Systems Center Pacific
Environmental Quality Branch

Distribution Statement A
This document has been cleared for public release

CONTENTS

1.0 Introduction 1

2.0 Maynord's Propeller Wash Model 2

2.1 Maynord's Model for Single Propeller 2

2.2 Maynord's Model for Twin-Screw Propeller 3

2.3 Bottom Shear Stress 5

2.4 Application of Maynord's Model for San Diego Bay 6

2.4.1 Critical Shear Stress and Empirical Erosion Constant 9

2.4.2 Sediment Erosion Rate 10

2.4.3 Comparison of Field Data and Model Results 12

3.0 Summary 15

4.0 References 15

Appendix A. Thrusts on nozzle propellers of the Tractor C-14 tugboat from measurements and the FANS model A-1

Appendix B. Graphic Maynord's Model output file and format B-1

Appendix C. Instructions on Running the Standalone Maynord Model on a 32-bit Microsoft® Windows® 7 Computer C-1

Appendix D. Instructions on Running the Standalone Maynord Model on a 64-bit Microsoft® Windows® 7 Computer D-1

TABLES

Table 1. Key model input parameters for the Graphic Maynord's Model. 8

Table A-1. Propeller information and operating conditions for ducted propeller..... 1

Table A-2. Comparison of the calculated thrust and torque coefficients (in confined water) with the experimental data (open water) under bollard-pull condition. 3

FIGURES

Figure 1. Schematic plots of twin-nozzle propellers for a tugboat in water of confined depth. 4

Figure 2. Field study of tugboat propeller wash in Pier 4-5 of San Diego Bay (configuration of instruments in propeller plume, left, and tugboat Tractor C-14, right). 7

Figure 3. Tugboat propeller speed during the field study (Hour 13.847-14.439, July 19, 2012). 7

Figure 4. Graphical Maynord's model with input window and output graphics (right panels). 8

Figure 5. Sample images taken (a) when there was no significant erosion; (b)-(e) at the inception of erosion (f) after continuous erosion and resuspension. 10

Figure 6. PIV images with visible sediment bed. The red line is the reconstructed bottom line. 11

Figure 7. Cumulative erosion depth measured form PIV image analysis and modeling results with bottom shear stress obtained from ADV data. 12

Figure 8. Comparison of velocity amplitudes for four propeller speeds between measurements and model results. 13

Figure 9. Bottom shear stress from model results and estimation calculated based on measured velocity field during the propeller wash experiment. 14

Figure 10. Cumulative shear stress over time between model results and estimation based on measured velocity field during the propeller wash experiment. 14

Figure A-1.Ducted propeller geometry. A-1

Figure A-2. Pressure distributions on the propeller blade, shaft and duct surfaces. A-2

Figure B-1. MATLAB Model GUI for the Graphic Maynord's Model. B-1

Figure B-2. Graphic interface of model input and output of the Graphic Maynord's Model. B-2

Figure B 3. Format of the output file (velocity field). B-3

Abstract

Resuspension of sediment by propeller wash has been an issue that requires scientific research and investigation for its impacts on management of contaminated sediments in DoD harbors. We have implemented the Maynord's model to predict velocity field, bottom shear stress and resuspension potential from propeller wash by a tugboat (Tractor C-14), which is of the same type of the Navy-contracted tugboats being used in many Navy harbors. The implementation includes both user-friendly input and output the model and validation of the model results by comparing with the field data. Characteristics and dimensions of the twin-engine tugboat propellers provide model input. Model-predicted velocity fields and shear stresses were compared with measured values from the field study. For erosion by propeller wash, the graphic Maynord's model uses the erosion rate constant and the critical shear stress, both obtained empirically from the field study, to predict erosion rate by propeller wash. With validation of the Maynord's model and the user-friendly model input/output, one can use the graphic Maynord's model for propeller wash and related studies in DoD harbors.

1.0 Introduction

Propeller wash produces significant disturbances of flow that induce resuspension of bottom sediment. Images of sediment plumes by propeller wash can be found on Google Earth throughout the U.S. ports and harbors as well as in the coastal water bodies around the world. Contaminated sediment is subject to a number of physical and chemical processes after resuspension in the water column. The transport process is governed by hydrodynamics, including current velocity and water volume variations, and turbulent mixing in the wake of the propeller. In addition to the hydrodynamic transport and turbulent mixing, contaminants (metals) and sediments are subject to settling. Partitioning of metals is also associated with the loss rate of metals from the transport and settling.

As part of the "Evaluation of Resuspension from Propeller Wash in DoD Harbors" project (ESTCP Project No. ER-201031), several numerical models were implemented and applied to simulate both the propeller wash resuspension process and the fate and transport process of resuspended plumes. This report discusses the application of the Maynord's propeller wash model to tugboat-induced resuspension at Pier 4-5, Naval Base San Diego, in San Diego Bay, CA.

For this study, we applied both field study and modeling simulations to evaluate flow field and shear stress induced by propeller wash near the bed. For the field study, an underwater Particle Image Velocimeter (PIV) measured the instantaneous velocity field at high-frequency and high spatial resolution near the bottom, including the bottom boundary layer region. A number of fluid parameters, including fluctuating velocity, energy dissipation rate, and Reynold's stress (as a surrogate to the bottom shear stress) can be directly measured (Liao et al., 2009). There are no other methods that can measure these parameters simultaneously in the field. Simultaneous deployment of the PIV with a Sediment Profiler Imagery (SPI) device and an Acoustic Doppler Current Profiler (ADCP) provided a relationship between the sediment erosion rate, bed stress and the mean near-bed velocity distribution specifically for the propeller wash. To establish this relationship, we also explored higher statistical moments of the measured Reynolds stress, or energy dissipation rate (i.e., variance, skewness) that accounts for peak bed stress in addition to the mean value. The main purpose of these measurements was to provide "ground-truth" data that did not exist until this study. These results were used to modify and calibrate the Maynord's model.

Maynord's model (1984) is one of the few models that have been used to predict flow velocities and shear stresses near the sediment bed induced by a propeller. The model was initially developed for a single-screw propeller operating in an infinite flow domain and is approximated for deep water applications. For the current study, most traffic and propeller wash for Navy/DoD vessels are shallow water, high-energy activities, and Maynord's model has been implemented for this environment and was used to estimate the bed shear stress at the sediment bed induced by the propeller wash. Bed shear stress is the most important parameter that determines both the inception of resuspension (the critical shear stress) and the entrainment rate. Existing models for propeller wash, i.e., Maynord's model (Maynord 1984, 1998; Maynord et al., 2006), predict near-bed velocity that is then converted to a bed shear stress. This conversion is based on turbulent boundary layer theory in channel flows, usually under a uniform and steady flow condition. Similarly, the U.S. Army Corps of Engineers High Shear Stress flume (SEDflume) was utilized to establish the relationship between the erosion rate and the varying near-bed flow velocity in a confined channel where flow is relatively uniform. Almost all existing sediment entrainment models are obtained through laboratory flume studies with well-defined flow conditions. However, the flow field behind a propeller is extremely turbulent and unsteady, making it a special case that differs significantly from flow fields found in channels rivers, tidal current, flood flow, wind waves, etc.

2.0 Maynord's Propeller Wash Model

2.1 Maynord's Model for Single Propeller

Maynord's model is based on the empirical model developed by Blaauw and van de Kaa (1978), which follows the law of conservation of momentum. The power of the rotating propeller is equal to the momentum of the flow field in the wake of the propeller. The propeller-induced velocity can be expressed explicitly as:

$$U(x,z) = AU_0\left(\frac{D_0}{x}\right)e^{-B\left(\frac{z}{x}\right)^2}, \qquad (1)$$

where x is the distance along the axial direction and z is the radial distance of the propeller (Figure 1). D_0 is the equivalent propeller diameter, and U_0 is the exit velocity of the propeller, which can be approximated by the power and diameter of the propeller (Blaauw and van de Kaa, 1978):

$$U_0 = C\left(\frac{P}{D_P}\right)^{1/3}, \qquad (2)$$

where C is an empirical constant, P the engine power of the propeller in [horse power], and Dp is the propeller diameter.

In Eq. (1), the two coefficients (constants), A and B, are obtained empirically. The model is for single-screw propellers in infinite flow domain. The velocities at the bottom are calculated by assigning the position (x, z) of the bottom to the equation, which means that the bottom is treated as a virtual bottom (transparent) in the model and the bottom effect to the hydrodynamics of the propeller wash is ignored. Maynord advised application of this method for propellers with the ratio of diameter/shaft-to-bottom distance D_p/H_p at low values (Figure 1), less than 1.2, to reduce the effects of the bottom (1998). However, most vessels in DoD harbors operate in very shallow water

conditions with D_p/H_p far exceeding 1.2 (e.g., aircraft carriers, destroyers, etc.). For the destroyer (DDG) test case considered in the preliminary investigation, the ship draft was 31 ft and the water depth was 35 ft. The diameter of the twin-screw propeller was D_p = 17 ft, and the distance from propeller shaft to harbor bottom was H_p = 15.3 ft. This gives D_p/H_p = 1.11, which is near the threshold applicable range of Maynord's model. However, there is a strong interaction between the two counter-rotating propellers. Consequently, the bottom shear-stress distribution is drastically different from that induced by a single-screw propeller. We conducted a literature search and we could not find many published manuscripts/data for validation of Maynord's model for the scenarios, $D_p/H_p > 1.2$, which is more applicable for naval vessels operating in DoD harbors. In the application of Maynord's model (Maynord, 1998), two examples were discussed in the study of sand particle sizes for protecting the sediment caps for a commercial vessel traffic and a recreational vessel traffic.

For both applications, the ratios of D_p/H_p are less than 1.2, within the applicable range for Maynord's model. The range of applicability for Maynord's model is also emphasized by Jay (2002), where he suggested that Maynord's model should be applied only for deep water scenarios with a small D_p/H_p ratio, with best results from smaller ratios. The bottom effect would be reduced by limiting application of the model to deep water, which is presumably more conformal to the model. However, for deep water scenarios, the propeller is closer to the free surface than to the bottom. Thus, the propeller jet should hit the free surface earlier than the bottom. The free surface effect would attenuate the propeller wash flow, and interfere with the conservation of momentum principle, on which Maynord's model is based (Blaauw and van de Kaa, 1978; Maynord, 1984).

2.2 Maynord's Model for Twin-Screw Propeller

Maynord (2000) presented two models to compute velocity magnitude near the sediment bed behind twin-screw propellers (tugboat). In these models, empirical values were measured for several model parameters. For this effort, our field study was conducted for tugboat pushing only in a stationary condition; therefore, the model for a stationary tugboat pushing condition is applied and presented. Figure 1 shows configurations of the twin-nozzle propellers from a side view (upper) and plane view (lower). Propeller-induced flows can be described in two zones, Zone 1 and Zone 2. Zone 1, less than 10 propeller diameters behind the propellers, includes the regions dominated by the jet flow from the propeller which is between the propeller and the end of transition distance ($X_p/D_p < 10$). Zone 2, greater than 10 propeller diameters behind the propellers, is dominated by the fully developed propeller flow, as described by Eqs. (3) and (4).

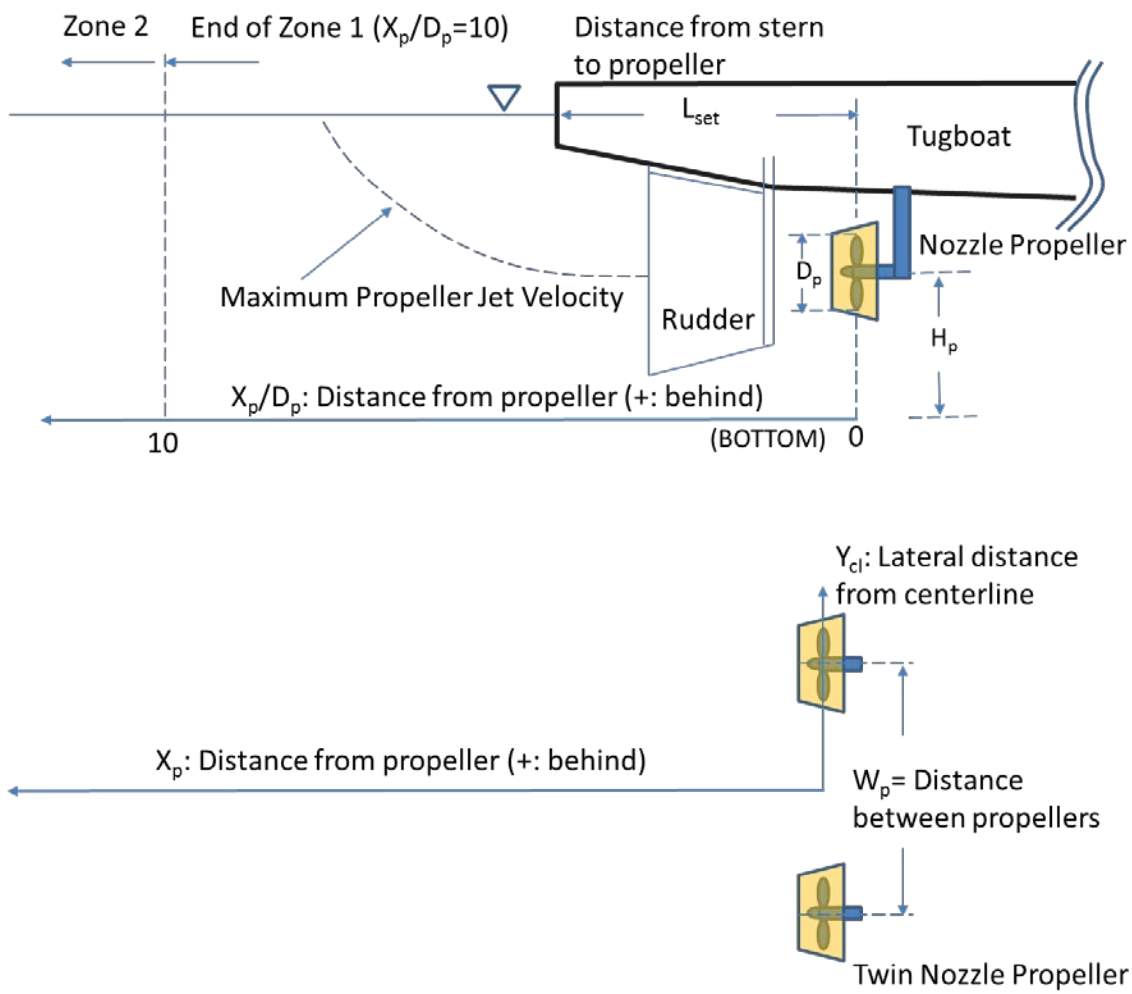

Figure 1. Schematic plots of twin-nozzle propellers for a tugboat in water of confined depth.

Maynord model calculation of the flow field in Zone 1:

$$V_1(X_p, Y_{cl}) = AX_p^{-0.524}\left[e^{\frac{-15.4R_1^2}{X_p^2}} + e^{\frac{-15.4R_2^2}{X_p^2}}\right] \qquad (3)$$

Maynord model calculation of the flow field in Zone 2:

$$V_2(X_p, Y_{cl}) = 0.34V_2C_1\left(\frac{D_p}{H_p}\right)^{0.93}\left(\frac{X_p}{D_p}\right)^{0.24} e^{-\left(\frac{0.0178X_p}{D_p}+\frac{Y_{cl}^2}{2C_{Z2}^2X_p^2}\right)} \qquad (4)$$

where:

$$A = 1.45V_2D_p^{0.524}$$

$$R_1^2 = \left(Y_{cl} - 0.5W_p\right)^2 + \left(H_p - C_j\right)^2$$

$$R_2^2 = \left(Y_{cl} + 0.5W_p\right)^2 + \left(H_p - C_j\right)^2$$

$C_j = -\left[0.213 - 1.05\left(\frac{C_p g}{V_2^2}\right)\left(X_p - 0.5L_{set}\right)\right]\left(X_p - 0.5L_{set}\right)$ = vertical distance from propeller shaft to location of maximum velocity within the jet, in meters

$$V_2 = \frac{1.13}{D_0}\sqrt{\frac{T}{\rho_w}}$$

T = Thrust of each propeller, N

$$C_p = \begin{cases} 0.12\left(\frac{D_p}{H_p}\right)^{0.67} & for\ open\ wheel\ propeller \\ 0.04 & for\ Kort\ nozzle\ propeller \end{cases}$$

$$D_0 = \begin{cases} 0.71D_p & for\ open\ wheel\ propeller \\ D_p & for\ Kort\ nozzle\ propeller \end{cases}$$

and,

X_p = Distance behind the propellers, m

Y_{cl}= Lateral distance from ship centerline, m

D_p= Propeller diameter, m

W_p= Distance between the twin propellers, m

L_{set}= Distance from ship stern to propeller, m

H_p = Distance from center of propeller axis to bottom, m

ρ_w=Density of water, Kg/m^3

2.3 Bottom Shear Stress

According to Maynord (2000), the bottom shear stress induced by the velocity field from the propellers can be calculated from Eq. (5):

$$\tau = 0.5\rho_w C_{fs} V_{prop}^2 \qquad (5)$$

where:

$$C_{fs} = 0.01\left(\frac{D_p}{H_p}\right)$$

and:

C_{fs} = bottom friction factor for propeller wash

τ = bottom shear stress (N/m^2)

V_{PROP} = bottom velocity (m/s)

Erosion for cohesive sediment has been modeled based on the relationship between bottom shear stress and critical shear stress. When the bottom shear stress exceeds the critical shear stress of the bed, erosion occurs. The erosion rate can be simulated by the following equation:

$$E = \begin{cases} 0, & \tau < \tau_{cr} \\ a(\tau - \tau_{cr})^n, & \tau \geq \tau_{cr} \end{cases} \qquad (6)$$

where E is the mass erosion rate with a dimension of [g m^{-2} s^{-1}]; α is the erosion rate constant, τ_{cr} is the critical shear stress, and n = 1 or 2. A linear relation (n = 1) was recommended for cohesive sediment by Kandiah (1974), while Lee et al. (2004), found n = 2 in their laboratory erosion experiments with undisturbed sediment cores from the Sheboygan River, WI.

Maynord (2000) introduced two forms of erosion rate formulae. Those two sets of equations are mathematically equivalent, and both are equivalent to Eq. (6), above, with n = 1 (empirically obtained for this study). It should be noted that the two erosion equations in Maynord (2000) and Eq. (6), above, may have different units for the erosion constant.

2.4 Application of Maynord's Model for San Diego Bay

In the field study, a Navy-contracted tugboat (Tractor C-14, Figure 2) was used to provide the propeller wash under controlled conditions. The tugboat was moored at Pier 4-5 with the bow pushing against the pier wall and the propellers thrusting toward the pier water. The tugboat has twin-nozzle propellers and Table 1 lists the dimensions of the tugboat and the propellers. At 110 meters behind the tugboat, a PIV and an Acoustic Doppler Velocimeter (ADV) were mounted to a frame which was placed on the bottom before the experiment started. The PIV measured the water velocity profile near the bottom (0-15 cm), and the ADV measured the water velocity at 15 cm above the bottom, during the study period of 13.847-14.44 hours (since 00:00AM July 19, 2012).

The propellers were operated at four speeds (Figure 3), starting at 20 rpm for 5 minutes, the lowest rpm possible without stalling the engine). Speed was then increased to 50 rpm for about 11 minutes, followed by subsequent increase to 100 RPM for about 9 minutes and 150 rpm for about 8 minutes. These four speeds were estimated by the operator/driver of the tugboat, and include estimates of uncertainty. The operator/driver estimated these uncertainties to be relatively larger for low speeds and lower for high speeds.

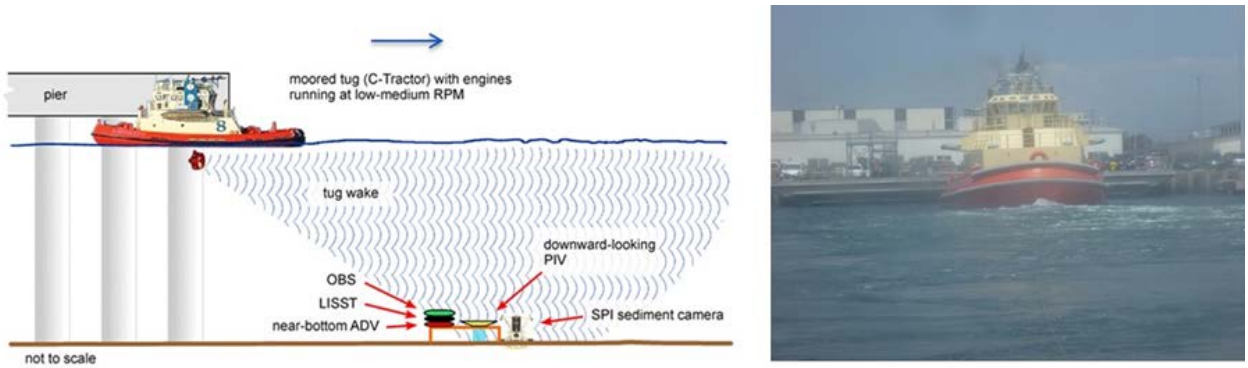

Figure 2. Field study of tugboat propeller wash at Pier 4-5 of Navy Base San Diego (configuration of instruments in propeller plume, left, and tugboat Tractor C-14, right).

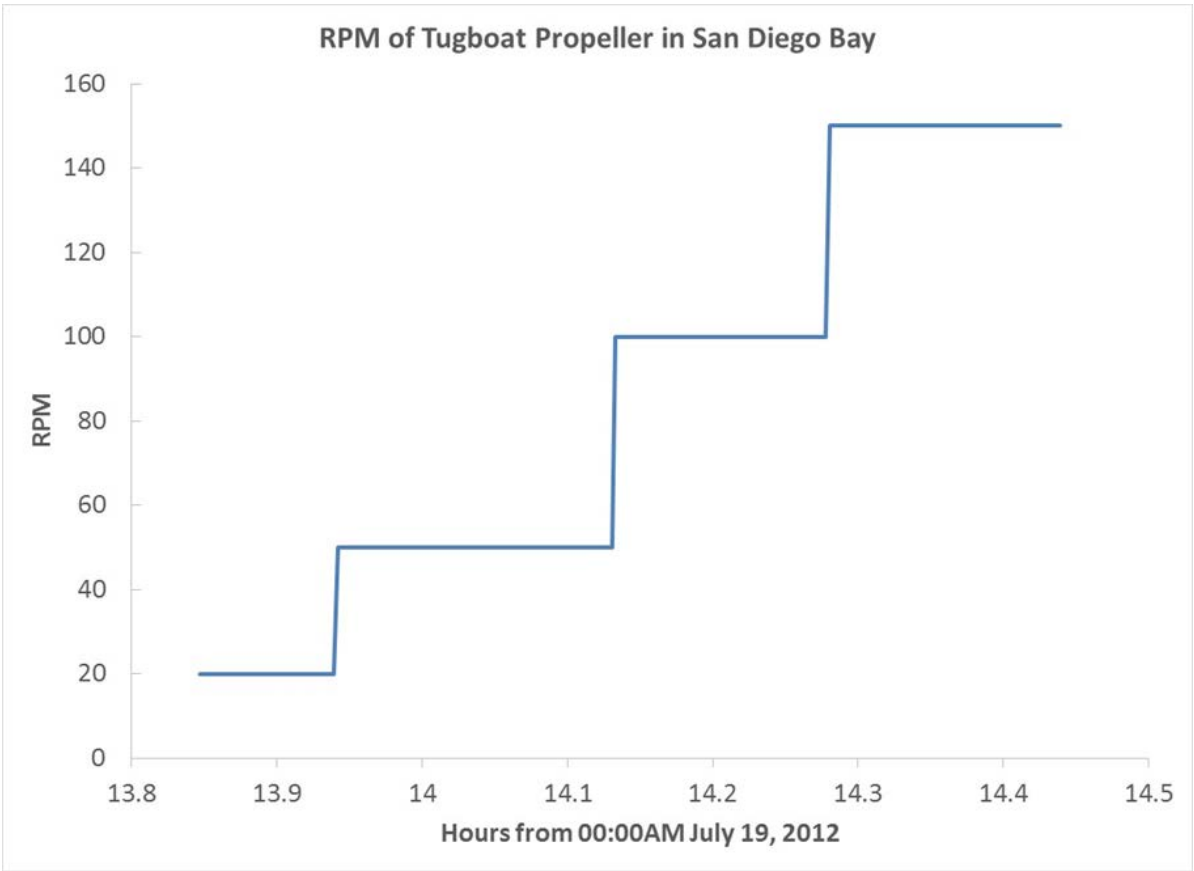

Figure 3. Tugboat propeller speed during the field study (Hours 13.847-14.439, July 19, 2012).

A user-friendly graphic version of Maynord's model has been developed (Figure 4) for the twin-engine tugboat. Input parameters for the model include propeller type (Kort nozzle or traditional), propeller diameter, thrust, shaft to bottom distance and water depth (Figure 1). The model calculates velocity profiles and shear stress at the bottom sediment bed. Both visual output and ASCII data files are produced. Table 1 lists the input parameters for the graphic Maynord's model.

Table 1. Key model input parameters for the Graphic Maynord's Model.

Parameter	Variables	Values
Distance between two propellers	D_p	2.28m
Distance from stern to propeller	L_{set}	15.24m
Center of propeller to bottom	H_p	4.267m
Thrust on each propeller(plus nozzle)	T at 20 rpm (propeller)	1,228 Newtons
	T at 50 rpm (propeller)	7,673 Newtons
	T at 100 rpm (propeller)	30,773 Newtons
	T at 150 rpm (propeller)	69,466 Newtons
Propeller spacing	Wp	4.877m
Erosion constant	a	15.7g/(m^2-sec-Pa)
Critical shear stress	τ_{cr}	0.47 (Pa)

The first three model parameters are associated with the tugboat and the propellers. These numbers were provided by the driver of the tugboat, which should be considered as estimates with uncertainties. During the study, the propellers of the tugboat were operated running at four different speeds, described above, with each speed maintained for 8-9 minutes.

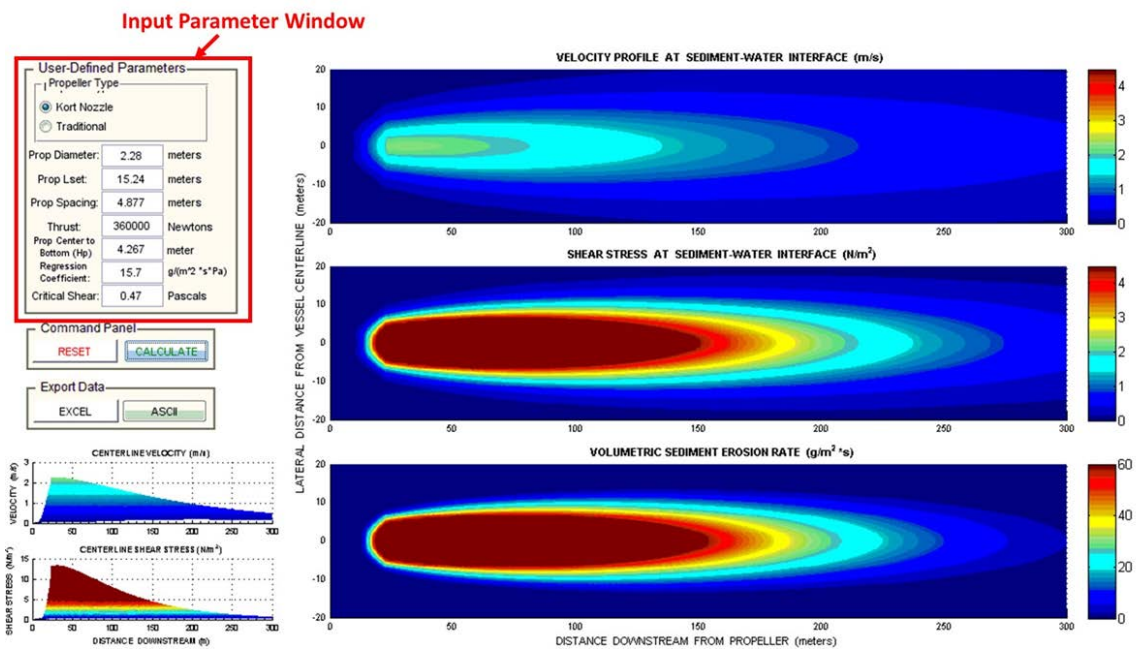

Figure 4. Graphical Maynord's model with input window and output graphics (right panels).

Thrusts on the propeller were estimated using a Finite Analytical Navier Stokes (FANS) model to simulate the tugboat operation at Pier 4-5. The propeller of the tugboat is Ka4-70 and the nozzle is based on the observed dimensions and shape from the picture we took. The propeller, including both the blades and the nozzle, and the tugboat were numerically segmented and simulated for the four propeller speeds used in the field study, 20, 50, 100 and 150 RPM. Model results of the propeller

thrust were compared with experimental results of open-water for propeller Ka4-70 in duct 19A (Baltazar et al., 2012) and can be found in Appendix A.

2.4.1 Critical Shear Stress and Empirical Erosion Constant

Two parameters are needed to calculate erosion rate (Eq. (6)), the critical shear stress (τ_{cr}) and the empirical erosion constant, a. These two constants were measured from the field study.

The critical shear stress was determined by visually checking PIV images for the initiation of sediment entrainment. Figure 5 presents sample images (I) when there was no significant sediment resuspension (Figure 5(a)) (II) at the inception of sediment entrainment (Figure 5(b)-(e)) and (III) a short moment after resuspension (Figure 5(f)). It is relatively easy to identify the moment of the inception of erosion, as a high concentration of sediment can be observed forming a “wedge”-like structure when they are lifted up by the shearing flow. The “edge” or “front” separating the sediment-laden flow and the overlaying clear fluid is sharp and signifies wall layer turbulent “eddies" (Figure 5(b)-(e)). This suggests that the initial entrainment of sediment from the bed is largely due to the “ejection” of the low momentum near-bed fluid by “horse shoe” vortex structures, which are also major contributors to the Reynolds shear stress in boundary layer turbulent flows. Usually, several seconds after the observed inception of erosion, as the bed sediment was continuously eroded and resuspended, the enhanced scattering blocked the laser light and the image became blurred or completely dark (Figure 5(f)).

The critical shear stress was estimated by calculating the mean velocity profile over a 5-second period around the moment when the initiation of resuspension was observed. The log-law profile fitting was applied to estimate the shear velocity, u_*. The bottom shear stress was then calculated as $\tau = \rho u_*^2$. With the available data, four cases in total were found that matched the selection criteria for the estimation of critical shear stress when the propeller speed was between 20 and 50 rpm. They are represented by Figure 5(b)-(e). The estimated bottom shear stresses are also shown in these figures. It should be noted that the critical shear stress obtained in this way is also a statistical average, which may not represent the instantaneous shear stress that initiates the sediment resuspension. The estimated critical shear stress for the four selected cases varied from 0.32 to 0.60 (Pa) with a mean of 0.47 (Pa). Therefore the critical shear stress for erosion for this site was estimated as τ_{cr}=0.47 (Pa).

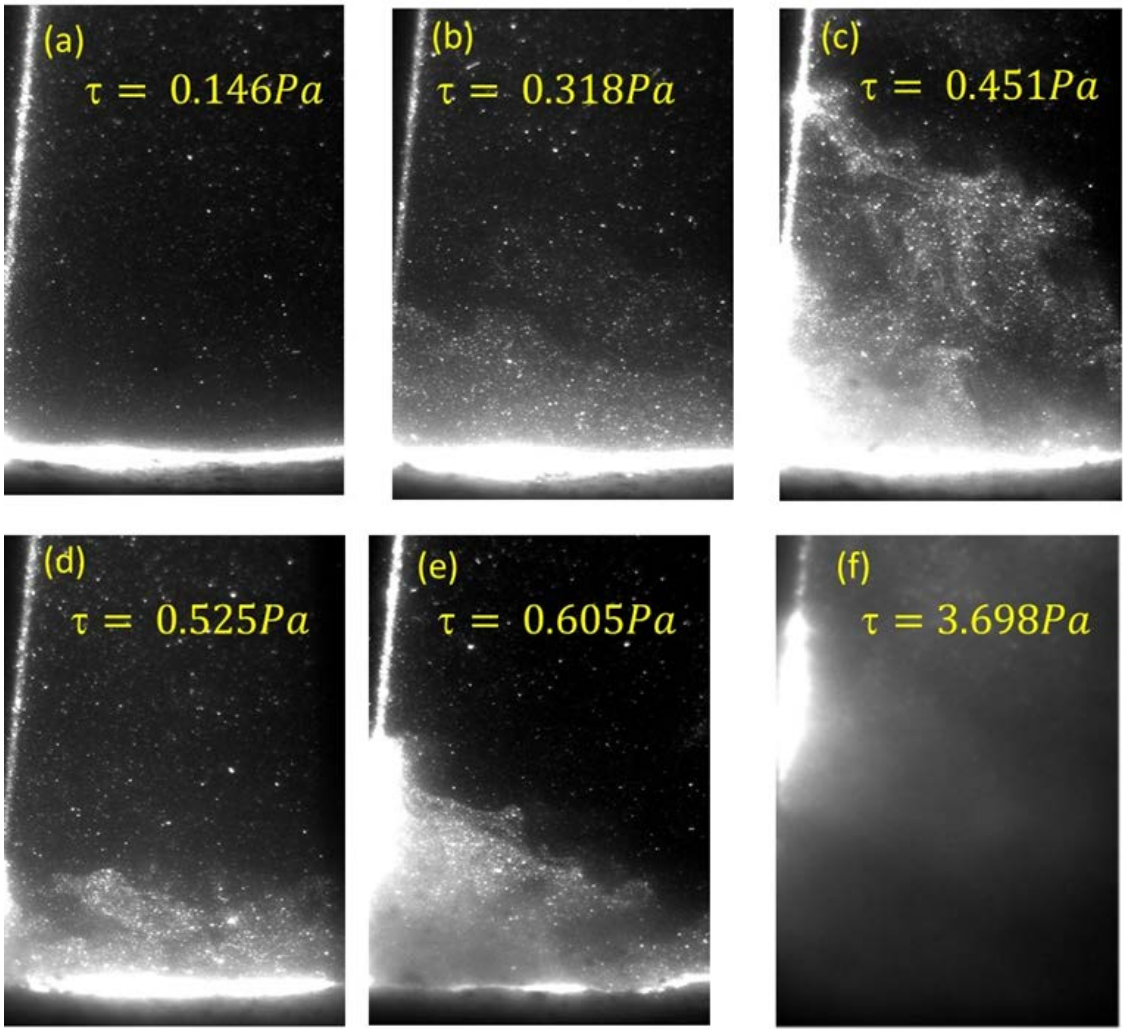

Figure 5. Sample images taken (a) when there was no significant erosion; (b)-(e) at the inception of erosion (f) after continuous erosion and resuspension.

2.4.2 Sediment Erosion Rate

Although most PIV images were blurred or completely dark with high sediment suspension at higher rpms, there were short moments when the sediment bottom became visible. We have selected some images (Figure 5) from the field results to evaluate the sediment erosion rate. Figure 6 shows combined images acquired at different times when the sediment bed was visible. From these images, we observed a continuous erosion of the bed before the propeller stopped at Hour 14.41. After that, the sediment bed rose up continuously, likely due to sediment deposition. From these images, we were able to estimate the change of sea bottom as a function of time with the assumption that the instrument platform was stable and did not sink.

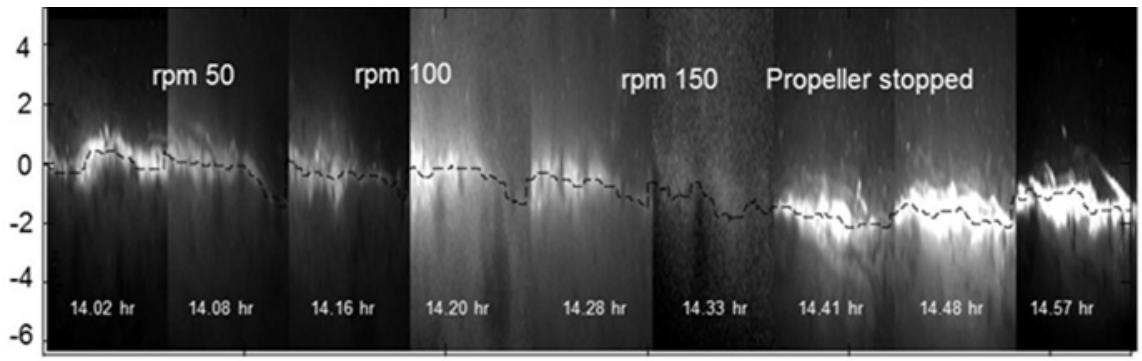

Figure 6. PIV images with visible sediment bed. The red line is the reconstructed bottom line.

The mass erosion rate can be converted to the depth erosion rate (E_D [m/s]) with the following relation:

$$E = \rho_b E_D \qquad (7)$$

where ρ_b is the dry bulk density of the sediment. Therefore the cumulative erosion depth can be modeled as

$$D(t) = \frac{a}{\rho_b}\int_0^t (\tau(t') - \tau_{cr})^{\alpha}\, dt' \qquad (8)$$

We applied Eq. (7) to fit the observed cumulative erosion depth in order to obtain the erosion rate constant a (Figure 7). Bottom shear stress was estimated with the covariance, TKE and modified TKE methods. The parameter $\frac{a}{\rho_b}$ was obtained through least squares fitting. The best results were found when we selected $n = 1$. Correlation coefficients (r^2) for the three methods were 51%, 56% and 93%, respectively. This suggests that bottom shear stress estimated from the modified TKE may be most reliable. The cumulative erosion depth and the model results from Eq. (8) are shown in Figure 7. Using the shear stress based on the modified TKE method, E_D = 0.0079[mm s^{-1} Pa^{-1})] ($\tau - \tau_{cr}$) [pa]. Taking a typical value for the dry bulk density of cohesive sediments, ρ_b=2000 (kg m^{-3}), the erosion rate constant α = 15.7 (g m^{-2} s^{-1} Pa^{-1}).

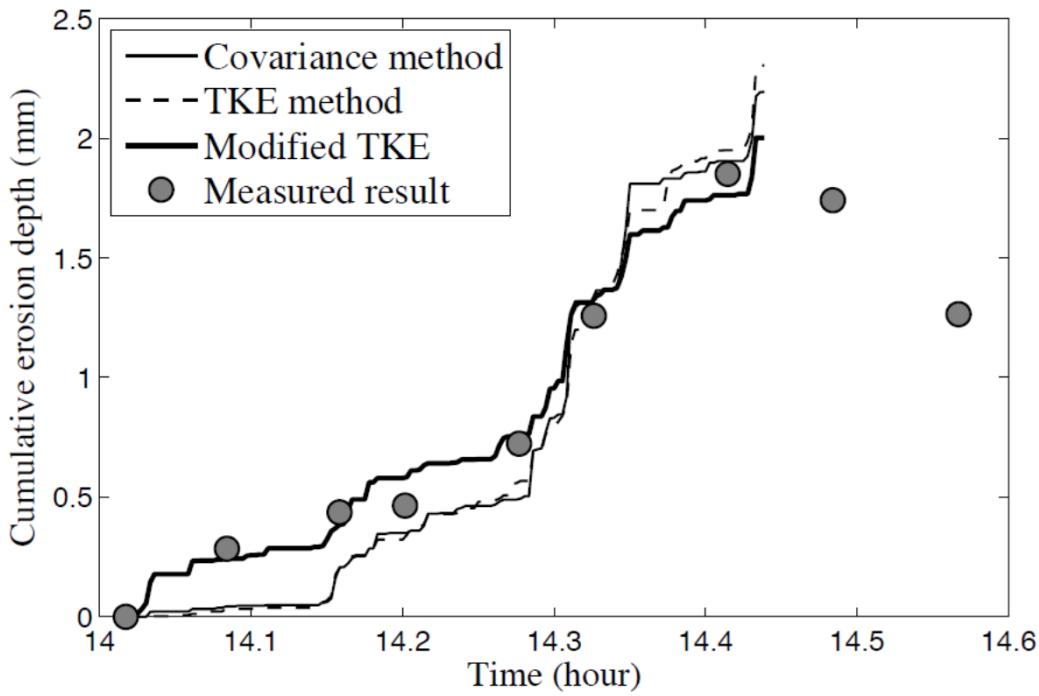

Figure 7. Cumulative erosion depth measured from PIV image analysis and modeling results with bottom shear stress obtained from ADV data.

2.4.3 Comparison of Field Data and Model Results

Figure 8 shows comparisons between the simulated and the measured velocity amplitudes near the bottom, at Pier 4-5, approximately 110m behind the tugboat. Velocity amplitudes were underestimated by the model when compared with field measurements for low propeller speeds at 20 rpm and 50 rpm. Simulated and measured velocity amplitudes were in good agreement for the 100 rpm case, but simulated velocities exceeded measured values for the 150 rpm scenario.

Simulated velocity amplitudes exhibited a linear relationship with the propeller speed, whereas our observed measurements showed non-linear behavior with increasing propeller speeds. Based on Eq. (4), velocity fields disturbed by propeller wash were proportional to the square root of thrust, $\sqrt{T}$, which is proportional to square of the propeller speed (n), $T \propto n^2$. Therefore, velocity amplitude was predicted to behave linearly with respect to the propeller speed, as shown by the model. The nonlinear relationship observed between velocity amplitude and propeller speed may be caused by multiple factors. For example, the restricted water domain in the pier may generate complex return flows and circulations associated with finite water depth. We note also that Maynord's model applies to open water scenarios, and was not originally intended for restricted water domain.

Under-prediction of velocity amplitudes by the model at low propeller speeds may be attributed to the driver's uncertainty in propeller speed estimates. The driver of the tugboat had difficulty in accurately operating the speed of the propeller and the maintaining control of the driving wheel at low speed. In addition, the driver had difficulty in maintaining 20 rpm propeller speed without stalling the engine. Actual propeller speeds for the 20 and 50 rpm field study may be underestimated; the actual propeller speeds are likely to be greater than 20 and 50 rpm, respectively.

Since there is no solid data to support these potential causes, we cannot comment reliably on the differences between the model and the measurements.

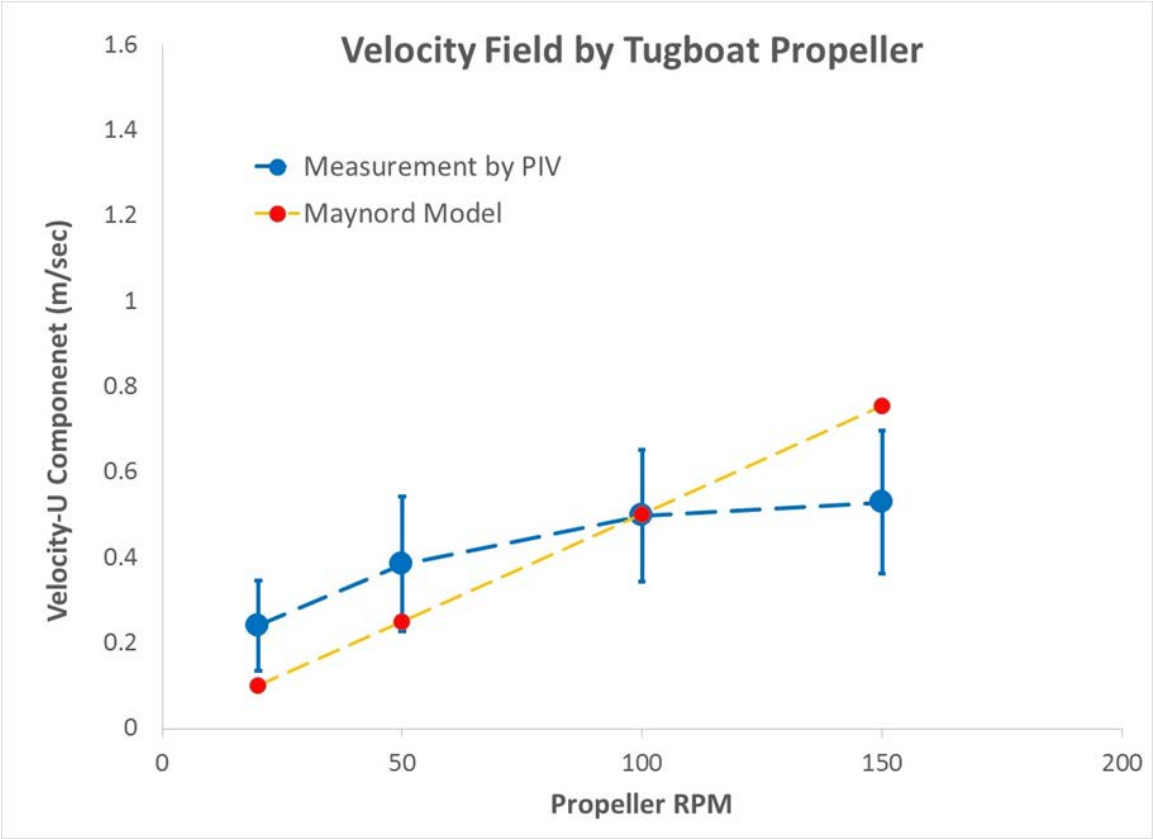

Figure 8. Comparison of velocity amplitudes for four propeller speeds between measurements and model results.

Bottom shear stress was calculated based on two sets of methods. The approach was based on the balance of total energy produced by the turbulence of the propeller wash and the dissipation by the bottom shear stress, which includes three different techniques to calculate bottom shear stress from the measured PIV velocity time series. The bottom shear stresses estimated from these three energy-balanced methods were compared with the shear stress calculated by the Maynord's model (Figure 9). It showed that Maynord's model under-estimates the bottom shear for propeller speeds at 20 rpm and 50 rpm, though this could have been due to the uncertainties discussed previously for the discrepancies in velocity prediction. For the 100 rpm and the 150 rpm cases, Maynord's model compared relatively well with those calculated by the energy balance methods.

Figure 10 shows the cumulative bottom shear stress over time, an integration of the shear stress curve shown in Figure 9. Cumulative shear stress provides overall effects of the shear stress including the mean and temporal variations over time. As shown in Figure 10, Maynord's model results under-predicted the cumulative effect compared with the estimated values from the three energy-balanced methods.

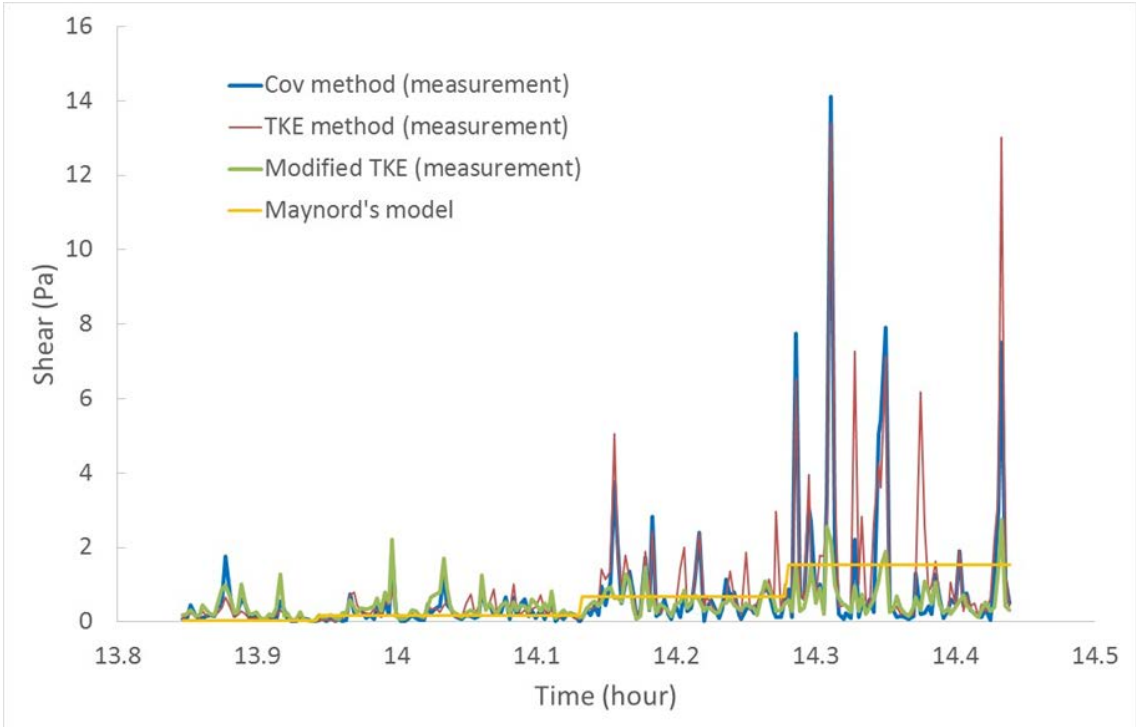

Figure 9. Bottom shear stress from model results and estimation calculated based on measured velocity field during the propeller wash experiment.

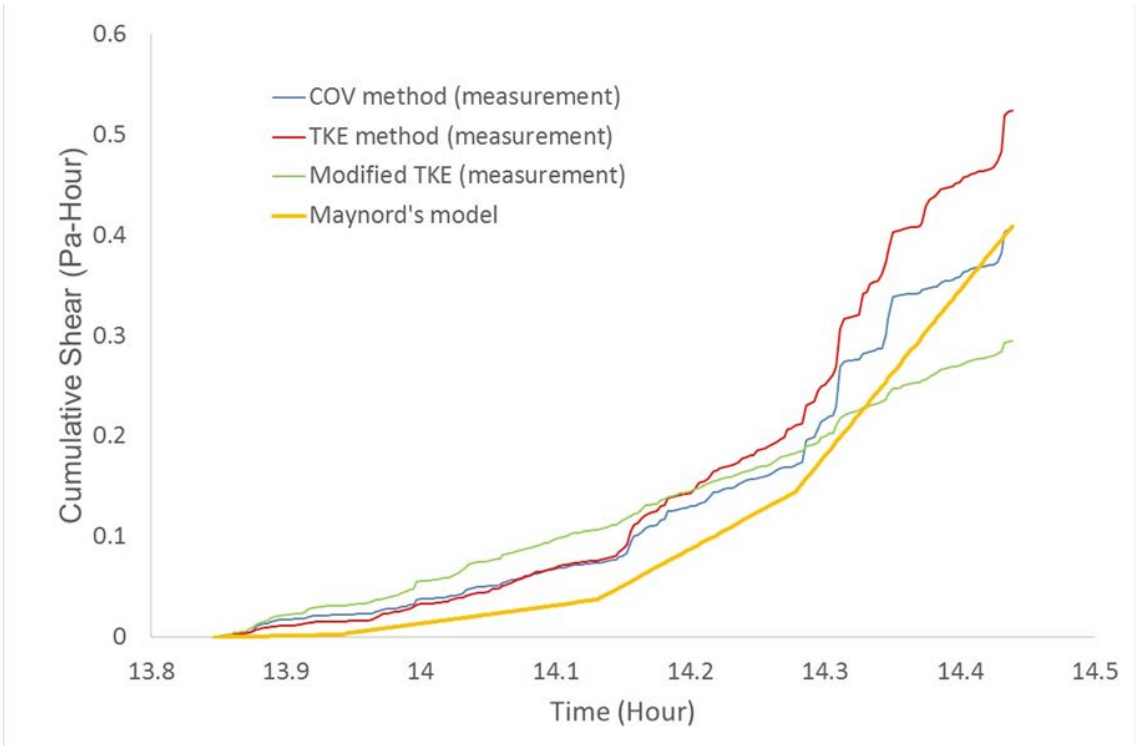

Figure 10. Cumulative shear stress over time between model results and estimation based on measured velocity field during the propeller wash experiment.

3.0 Summary

We have investigated analyzed and implemented Maynord's model (Maynord, 1984; 2000) for investigation of propeller wash in DoD harbors. As discussed, Maynord's model is based on the theory of conservation of momentum and implemented for propellers with a single engine (Maynord 1984) and twin propellers (Maynord 2000). While convenient, Maynord's model has its application limitation – namely, the ratio of propeller diameter to propeller-to-bottom distance, D_p/H_p, should be less than 1.2. Specifically, Maynord's model is applicable for propeller wash studies for tugboats and may not be applicable for deep-draft vessels, such as aircraft carriers and DDGs. Maynord's model was implemented with the user-friendly graphic model input and output interface (the "graphic Maynord's model"). The characteristics and dimensions of the tugboat propellers, including propeller diameters, distances between the propeller and the bottom, spacing of the propellers, horizontal distance between the stern and the propeller and the thrust on the propeller provide the first set of model input for prediction of velocity field and shear stress near the bottom. Thrusts on the propellers were predicted by the FANS model; and predicted thrusts were validated by the field measurements (Baltazar et al., 2012). Both predicted velocity field and predicted bottom shear stress compared fairly well with measured values. The graphic Maynord's model also requires critical stress and erosion rate constants. These were derived from the empirical values obtained from the field study . We demonstrated that the graphic Maynord's model, with its user-friendly model input/output interface and added capability of calculating erosion potential from propeller wash, and validated by the field data of velocity and shear stress, can be a useful tool for propeller wash and related studies in DoD harbors.

4.0 References

Baltazar, J., J.A.C. Falcao de Campos, and J. Bosschers, 2012, "Open-Water Thrust and Torque Predictions of a Ducked Propeller System with a Panel Method", *Int, J. Rotating Mach.*, Vol. 2012, Article ID 474785, 11 pages.

Blaauw, H. B. and E. J. Va de Kaa. 1978. "Erosion of Bottom and Sloping Banks caused by the Screw-race of Maneuvering Ships," Publication 202. Delft, The Netherlands.

Jay, David, 2002, "An Analysis of Propwash, Spillage and Sediment Transport Impacts of the Maury Island, Glacier Northwest Gravel Mine," Technical Report, OGI School of Science and Engineering, Oregon Health & Science University, Beaverton, OR.

Kandiah, A. 1974, Fundamental aspects of surface erosion of cohesive soils, Ph.D. thesis, Univ. of California at Davis, 1974.

Liao, Q., H. Bootsma, J. Xiao, J. Klump, A. Hume, M. Long, P. Berg, 2009, "Development of an in situ underwater particle image velocimetry (uwpiv) system", *Limnol. Oceanogr. Meth.* 7: 169-184 (2009).

Lee,C., C. Wu, J. Hoopes, 2004, Automated sediment erosion testing system using digital imaging, *J. Hydraul. Eng.* 130(8): 771-782.

Maynord, S., J. Hite, and M. Sanchez. 2006. "Atkinson Island Mooring Basin Alternatives, Houston Ship Channel." U.S. Army Corps of Engineers, Engineer Research and Development Center, Report CHLTR06-09, Vicksburg, MS.

Maynord, S. T. 1984. "Riprap Protection on Navigable Waterways." Technical Report HL-84-3. U.S. Army Engineers Waterways Experiment Station. Vicksburg, MS.

Maynord, S. T. 1998. “Guidance for In-Situ Subaqueous Capping of Contaminated Sediments: Appendix A: Armor Layer Design.” Technical Draft. U.S. Army Division for U.S. EPA.

Maynord, Stephen T. 2000. “Physical Forces Near Commercial Tows,” Interim Report, U.S. Army Engineer Research and Development Center, Vicksburg, MS 39180-6199.

Appendix A. Thrusts on nozzle propellers of the Tractor C-14 tugboat from measurements and the FANS model

To simulate the flow field induced by the twin-engine tugboat (Tractor C-14), we selected a typical ducted propeller with the four-bladed Ka4-70 propeller inside a 19A duct as shown in Figure A-1. The propeller specifications and the operating conditions are summarized in Table A-1. The FANS model was employed to calculate the thrust and torque produced by the ducted propeller at five different rotating speeds (20, 50, 100, 150 and 200 rpm) under bollard-pull conditions.

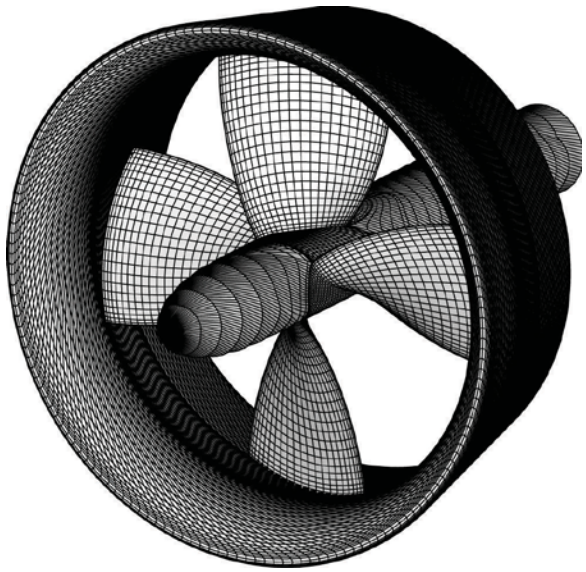

Figure A-1.Ducted propeller geometry.

Table A-1. Propeller information and operating conditions for ducted propeller.

Characteristics/Dimensions	1
Ship length L (m)	28.65 (94 ft)
Ship Beam B (m)	10.36 (34 ft)
Ship Draft (m)	3.353 (11 ft)
Water depth, H (m)	9.144 (30 ft)
Distance from ship bow to pier wall at waterline (m)	1.8288 (6 ft)
Distance from ship stern to pier wall at waterline (m)	30.48 (100 ft)
Clearance between ship sidewall and Pier wall (m)	Open water
Underkeel clearance (m)	2.997 (9.833 ft)
Propeller Diameter, D_p (m)	***2.286 (7.5 ft)***
Distance between Propellers (W_p) (m)	***4.8768 (16 ft)***

Table A-1. Propeller information and operating conditions for ducted propeller.

Distance from ship stern to propeller (L_{set}) (m)	***15.24 (50 ft)***
Propeller Depth (depth of the propeller axis) (m)	4.8768 (16 ft)
Distance from center of propeller axis to bottom (H_p) (m)	***4.2672 (14 ft)***
gap clearance between propeller duct and tugboat bottom (m)	***0.14 (0.46 ft)***
Ship speed (knots)	0
Propeller rpm, n	20, 50, 100, 150 and 200
Characteristic time, T_o (s)	0.3
Characteristic velocity U_o (m/s)	1.016
Reynolds number based on characteristic length L_o (= 1 ft)	2.647×10^5
Reynolds number based on propeller diameter D	1.488×10^7

Figure A-2shows the surface pressure distributions on the propeller blade, shaft and duct surfaces for the 100 rpm case. It should be noted that the pressure is normalized by $P_o = \rho n^2 D_p^2$, where ρ = 1030 kg/m^3 is the density of seawater, n is the propeller rotating speed, and D = 2.286 m (7.5 ft) is the propeller diameter. It is clearly seen from Figure A-2 that the propeller rotation induced a strong negative pressure on the suction side of the propeller blade and a relatively mild positive pressure on the pressure side. The net forces and torques acting on the ducted propeller can be obtained by numerical integration of the surface pressures and shear stresses over the blade, shaft, and duct surfaces. The dimensionless thrust and torque of the ducted propeller are given by the propeller thrust coefficient K_{TP}, the duct thrust coefficient K_{TD}, and the torque coefficient K_Q defined below:

$$K_{TP} = \frac{T_P}{\rho n^2 D^4}, \quad K_{TD} = \frac{T_D}{\rho n^2 D^4}, \quad K_Q = \frac{Q}{\rho n^2 D^5}$$

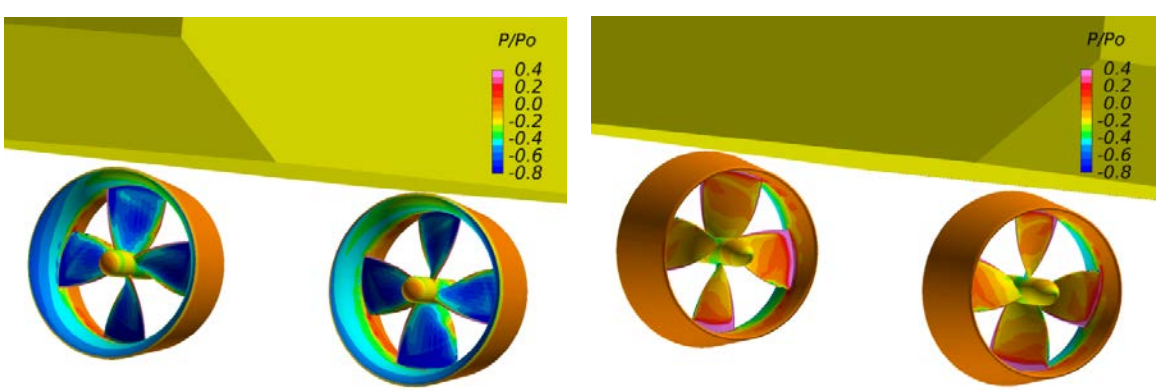

Figure A-2. Pressure distributions on the propeller blade, shaft and duct surfaces.

Table A-2 shows the calculated thrusts and torques for the ducted propeller at rotating speeds of 20 rpm, 50 rpm, 100 rpm, 150 rpm and 200 rpm. It was noted that the thrust and torque produced by the ducted propeller increase quadratically with the propeller rotating speed. With increasing propeller rotating speed from 20 to 200 rpm, the predicted propeller thrust coefficient K_{TP} increased slightly from 0.242 to 0.249 while the duct thrust coefficient K_{TD} reduced slightly from 0.151 to 0.147. The calculated propeller thrust coefficient K_{TP} was in excellent agreement with the experimental data. On the other hand, the predicted duct thrust coefficient K_{TD} was about 45% lower than the measured value of 0.27. The observed difference in K_{TD} can be attributed mainly to the blockage effect by the tugboat, and to a lesser degree the shallow water effect in a confined harbor. As noted in Table A-1, the minimum gap clearance between the propeller duct and the tugboat bottom is only 0.14 m (0.46 ft) or about 6% of the propeller diameter. It is clearly seen from Figure A-2 that the suction pressure on the duct inner surface is significantly weaker in the vicinity of the tugboat bottom surface due to the effect of narrow gap clearance. This resulted in a significant reduction of the thrust force acting on the duct compaired to open water conditions. Consequently, the total thrust force produced by the ducted propeller was about 20% lower in a confined harbor with the presence of tugboat and seabed boundaries.

For completeness, a comparison of the calculated and measured torque coefficients is provided in Table A-2. Torque coefficient reduces from 0.0483 to 0.0441 when the rotating speed was increased from 20 to 200 rpm, which is also in excellent agreement with the measured K_Q value of 0.045. The present simulation results indicate that the tugboat blockage and shallow water effects do not alter the overall performance of the propeller thrust (K_{TP}) and torque (K_Q) since the propeller is shielded inside the duct. However, the thrust force induced by the duct (nozzle) is significantly reduced as a result of the tugboat blockage.

Table A-2. Comparison of the calculated thrust and torque coefficients (in confined water) with the experimental data (open water) under bollard-pull condition.

	K_{TP}	K_{TD}	K_T	K_Q
Experiment (open water)	0.25 (propeller thrust)	0.27 (duct thrust)	0.52 (total thrust)	0.045 (total torque)
20 rpm	0.242 (756 N)	0.151 (472 N)	0.393 (1,228 N)	0.0483 (345 N-m)
50 rpm	0.243 (4,744 N)	0.150 (2,929 N)	0.393 (7,673 N)	0.0475 (2,123 N-m)
100 rpm	0.246 (19,240 N)	0.148 (11,533 N)	0.394 (30,773 N)	0.0454 (8,113 N-m)
150 rpm	0.248 (43,606 N)	0.147 (25,860 N)	0.395 (69,466 N)	0.0446 (17,940 N-m)
200 rpm	0.249 (77,763 N)	0.147 (45,982 N)	0.396 (123,745 N)	0.0441 (31,485 N-m)

Appendix B. Graphic Maynord's Model output file and format

This model was based on a study conducted by Donald F. Hayes et al., published in the Journal of Dredging Engineering (Vol. 12, No. 2, Oct. 2012) titled "Vessel-induced sediment resuspension". The goal of this modeling effort was to determine the significance of the impact on a predefined sediment bed caused by propeller-induced fluid turbulence. When propeller-induced fluid velocities produced a shear stress in excess of the critical shear for a given sediment type, sediment was entrained into the water column, and transported via advection.

Below are the quick procedures to run the model and generate model output:

1. The MATLAB® PropWash GUI will appear in a new window (Figure B-1)
2. Locate the '**User-Defined Parameters'** window (Figure B-2)
3. Insert the desired **parameters**
4. Locate the '**Command Panel**' window
5. Click '**Calculate**'
6. Locate Export Data
7. Click 'EXCEL' or 'ASCII'

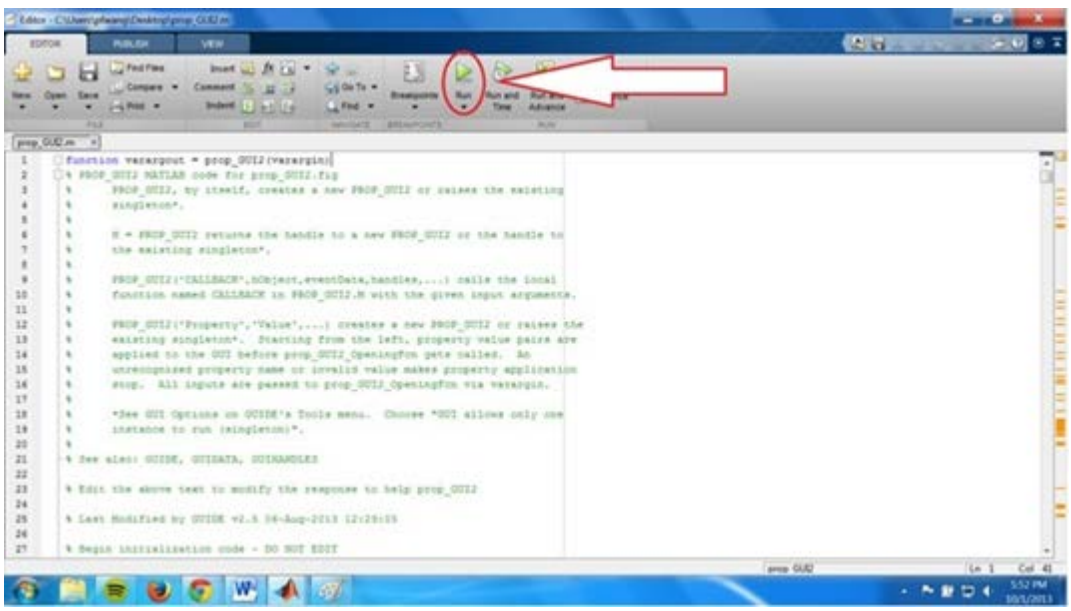

Figure B-1. MATLAB® Model GUI for the Graphic Maynord's Model.

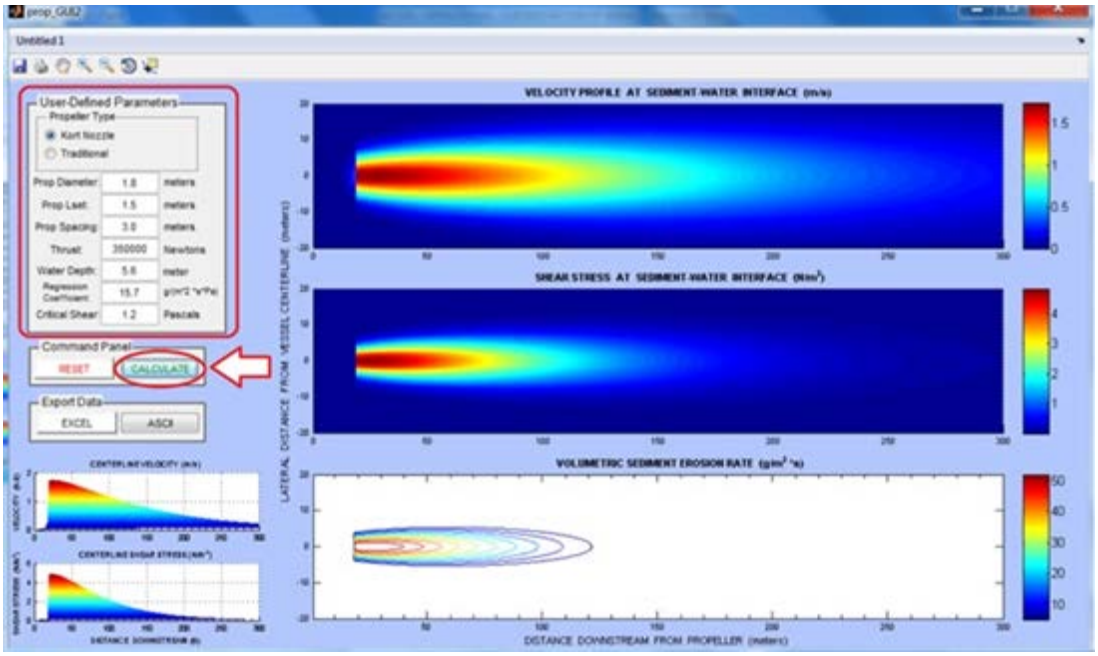

Figure B-2. Graphic interface of model input and output of the Graphic Maynord's Model.

Instructions on data export:

1. Run prop_GUI2_win*xx*.exe. A splash screen will appear while the prop_GUI application is loading.
2. Enter the desired User-Defined Parameters.
3. Click "Calculate" in the Command Panel. The contour plots on the bottom and right hand side will populate.
4. If the plots are satisfactory, click either "Excel" or "ASCII" to export the data in the desired format. Please wait until one data export process is complete before starting another. Make sure to click "Calculate" after any user-defined parameters are changed to ensure that the data is updated before it is exported. Clicking "Reset" will return the default User-Defined Parameters.
   a. The ASCII export option will create 4 comma delimited text files named prop_velocity.txt, prop_shear.txt, prop_erosion.txt, and prop_erosion2.txt in the same folder as prop_GUI2_winxx.exe resides. These text files can be opened later with Microsoft® Excel®.
   b. The Excel® export option will generate an Excel file named prop_data*[current date and time]*.xlsx. This file will have four sheets named, Sheet1, Sheet2, Sheet3, and Sheet4. It will reside in the same directory as prop_GUI2_win*xx*.exe. The four sheets contain velocity, shear, erosion, and erosion2 data. Please be patient. The Excel data export takes about 5 minutes. Please refrain from executing any other commands in the prop_GUI window during this time. A message box will notify you when the export is complete.

Exporting data directly into Excel® requires a considerable amount of time. It is much faster to export the data as ASCII files and open them in Excel®.

In the Excel® data file, Sheet 1 contains the velocity data. The first column of cells, A4:A84, contain the y data, the third row of cells, B3:WC3, contain the x data. The units of x and y are meters. Cells B4:WC84 contain the velocity data in m/s. Sheet 2 contains the shear stress data, in the same format

as the velocity (shear data is cells B4:WC4). The units of shear stress are Pascal. Sheet 3 contains the volumetric erosion rate data in grams/(m^2 *s).

Figure B 3 shows the format of the output file for velocity and shear stress near the bottom in the wake of the tugboat propellers.

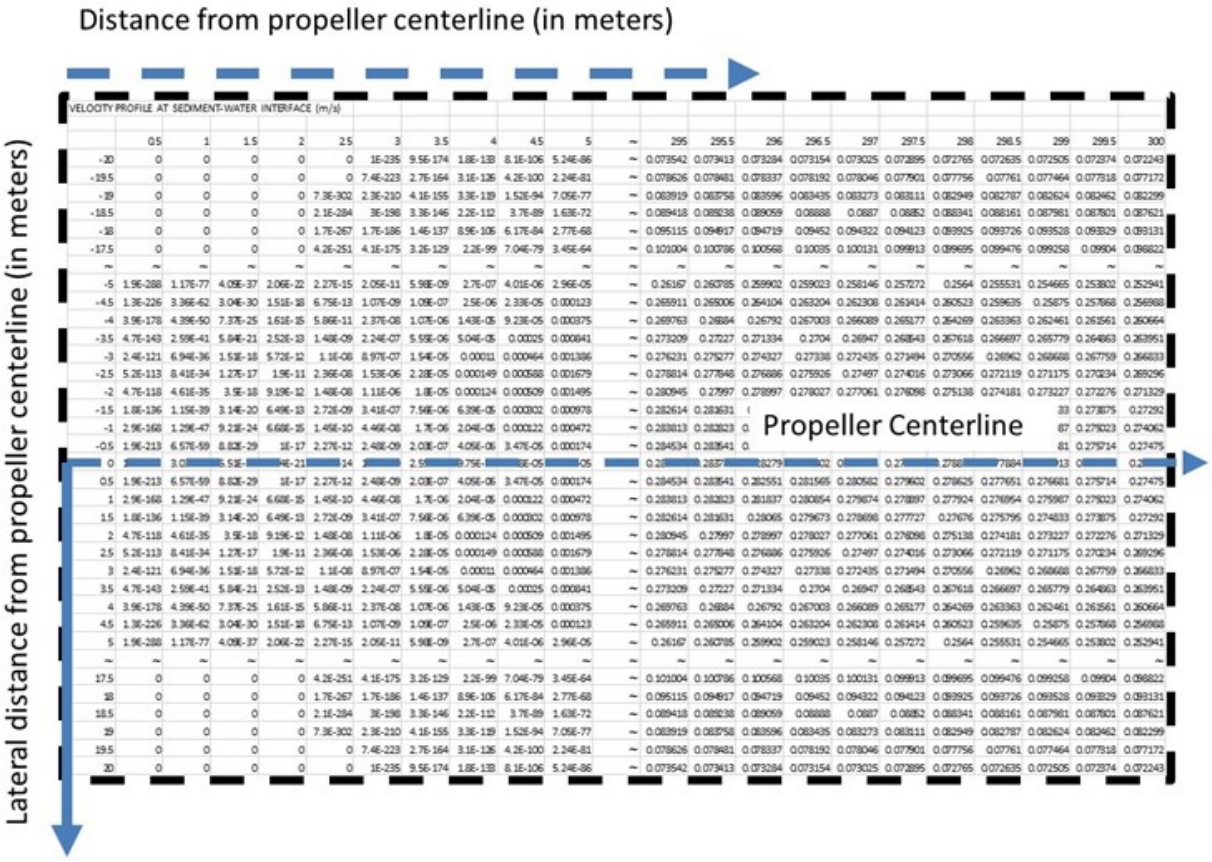

VELOCITY PROFILE AT SEDIMENT-WATER INTERFACE (m/s)

	0.5	1	1.5	2	2.5	3	3.5	4	4.5	5	~	295	295.5	296	296.5	297	297.5	298	298.5	299	299.5	300
-20	0	0	0	0	0	1E-235	9.5E-174	1.8E-133	8.1E-106	5.2E-86	~	0.073542	0.073413	0.073284	0.073154	0.073025	0.072895	0.072765	0.072635	0.072505	0.072374	0.072243
-19.5	0	0	0	0	0	7.4E-223	2.7E-164	3.1E-126	4.2E-100	2.2E-81	~	0.078626	0.078481	0.078337	0.078192	0.078046	0.077901	0.077756	0.07761	0.077464	0.077318	0.077172
-19	0	0	0	0	7.3E-302	2.3E-210	4.1E-155	3.3E-119	1.5E-94	7.05E-77	~	0.083919	0.083758	0.083596	0.083435	0.083273	0.083111	0.082949	0.082787	0.082624	0.082462	0.082299
-18.5	0	0	0	0	2.1E-284	3E-198	3.3E-146	2.2E-112	3.7E-89	1.63E-72	~	0.089418	0.089238	0.089059	0.08888	0.0887	0.08852	0.088341	0.088161	0.087981	0.087801	0.087621
-18	0	0	0	0	1.7E-267	1.7E-186	1.4E-137	8.9E-105	6.1E-84	2.7E-68	~	0.095115	0.094917	0.094719	0.09452	0.094322	0.094123	0.093925	0.093726	0.093528	0.093329	0.093131
-17.5	0	0	0	0	4.2E-251	4.1E-175	3.2E-129	2.2E-99	7.04E-79	3.45E-64	~	0.101004	0.100786	0.100568	0.10035	0.100131	0.099913	0.099695	0.099476	0.099258	0.09904	0.098822
~	~	~	~	~	~	~	~	~	~	~	~	~	~	~	~	~	~	~	~	~	~	~
-5	1.9E-288	1.17E-77	4.09E-37	2.06E-22	2.27E-15	2.05E-11	5.98E-09	2.7E-07	4.01E-06	2.96E-05	~	0.26167	0.260785	0.259902	0.259023	0.258146	0.257272	0.2564	0.255531	0.254665	0.253802	0.252941
-4.5	1.3E-226	3.36E-62	3.04E-30	1.51E-18	6.75E-13	1.07E-09	1.09E-07	2.5E-06	2.33E-05	0.000123	~	0.265911	0.265006	0.264104	0.263204	0.262308	0.261414	0.260523	0.259635	0.25875	0.257868	0.256988
-4	3.9E-178	4.39E-50	7.37E-25	1.61E-15	5.86E-11	2.37E-08	1.07E-06	1.43E-05	9.23E-05	0.000375	~	0.269763	0.26884	0.26792	0.267003	0.266089	0.265177	0.264269	0.263363	0.262461	0.261561	0.260664
-3.5	4.7E-143	2.59E-41	5.84E-21	2.52E-13	1.48E-09	2.24E-07	5.55E-06	5.04E-05	0.00025	0.000841	~	0.273209	0.27227	0.271334	0.2704	0.26947	0.268543	0.267618	0.266697	0.265779	0.264863	0.263951
-3	2.4E-121	6.94E-36	1.51E-18	5.72E-12	1.1E-08	8.97E-07	1.54E-05	0.00011	0.000464	0.001386	~	0.276231	0.275277	0.274327	0.27338	0.272435	0.271494	0.270556	0.26962	0.268688	0.267759	0.266833
-2.5	5.2E-113	8.41E-34	1.27E-17	1.9E-11	2.36E-08	1.53E-06	2.28E-05	0.000149	0.000588	0.001679	~	0.278814	0.277848	0.276886	0.275926	0.27497	0.274016	0.273066	0.272119	0.271175	0.270234	0.269296
-2	4.7E-118	4.61E-35	3.5E-18	9.19E-12	1.48E-08	1.11E-06	1.8E-05	0.000124	0.000509	0.001495	~	0.280945	0.27997	0.278997	0.278027	0.277061	0.276098	0.275138	0.274181	0.273227	0.272276	0.271329
-1.5	1.8E-136	1.15E-39	3.14E-20	6.49E-13	2.72E-09	3.41E-07	7.56E-06	6.39E-05	0.000302	0.000978	~	0.282614	0.281631	[illegible]	[illegible]	[illegible]	[illegible]	[illegible]	[illegible]	33	0.273875	0.27292
-1	2.9E-168	1.29E-47	9.21E-24	6.68E-15	1.45E-10	4.46E-08	1.7E-06	2.04E-05	0.000122	0.000472	~	0.283813	0.282823	0.	[illegible]	[illegible]	[illegible]	[illegible]	[illegible]	67	0.275023	0.274062
-0.5	1.9E-213	6.57E-59	8.82E-29	1E-17	2.27E-12	2.48E-09	2.03E-07	4.05E-06	3.47E-05	0.000174	~	0.284534	0.283641	0.	[illegible]	[illegible]	[illegible]	[illegible]	[illegible]	81	0.275714	0.27475
0	[illegible]	3.0[illegible]	[illegible]	[illegible]	[illegible]	[illegible]	[illegible]	[illegible]	[illegible]	[illegible]	~	0.2[illegible]	0.283[illegible]	[illegible]	[illegible]	0[illegible]	2[illegible]	[illegible]	[illegible]	[illegible]	0[illegible]	0.2[illegible]
0.5	1.9E-213	6.57E-59	8.82E-29	1E-17	2.27E-12	2.48E-09	2.03E-07	4.05E-06	3.47E-05	0.000174	~	0.284534	0.283641	0.282551	0.281565	0.280582	0.279602	0.278625	0.277651	0.276681	0.275714	0.27475
1	2.9E-168	1.29E-47	9.21E-24	6.68E-15	1.45E-10	4.46E-08	1.7E-06	2.04E-05	0.000122	0.000472	~	0.283813	0.282823	0.281837	0.280854	0.279874	0.278897	0.277924	0.276954	0.275987	0.275023	0.274062
1.5	1.8E-136	1.15E-39	3.14E-20	6.49E-13	2.72E-09	3.41E-07	7.56E-06	6.39E-05	0.000302	0.000978	~	0.282614	0.281631	0.28065	0.279673	0.278698	0.277727	0.27676	0.275795	0.274833	0.273875	0.27292
2	4.7E-118	4.61E-35	3.5E-18	9.19E-12	1.48E-08	1.11E-06	1.8E-05	0.000124	0.000509	0.001495	~	0.280945	0.27997	0.278997	0.278027	0.277061	0.276098	0.275138	0.274181	0.273227	0.272276	0.271329
2.5	5.2E-113	8.41E-34	1.27E-17	1.9E-11	2.36E-08	1.53E-06	2.28E-05	0.000149	0.000588	0.001679	~	0.278814	0.277848	0.276886	0.275926	0.27497	0.274016	0.273066	0.272119	0.271175	0.270234	0.269296
3	2.4E-121	6.94E-36	1.51E-18	5.72E-12	1.1E-08	8.97E-07	1.54E-05	0.00011	0.000464	0.001386	~	0.276231	0.275277	0.274327	0.27338	0.272435	0.271494	0.270556	0.26962	0.268688	0.267759	0.266833
3.5	4.7E-143	2.59E-41	5.84E-21	2.52E-13	1.48E-09	2.24E-07	5.55E-06	5.04E-05	0.00025	0.000841	~	0.273209	0.27227	0.271334	0.2704	0.26947	0.268543	0.267618	0.266697	0.265779	0.264863	0.263951
4	3.9E-178	4.39E-50	7.37E-25	1.61E-15	5.86E-11	2.37E-08	1.07E-06	1.43E-05	9.23E-05	0.000375	~	0.269763	0.26884	0.26792	0.267003	0.266089	0.265177	0.264269	0.263363	0.262461	0.261561	0.260664
4.5	1.3E-226	3.36E-62	3.04E-30	1.51E-18	6.75E-13	1.07E-09	1.09E-07	2.5E-06	2.33E-05	0.000123	~	0.265911	0.265006	0.264104	0.263204	0.262308	0.261414	0.260523	0.259635	0.25875	0.257868	0.256988
5	1.9E-288	1.17E-77	4.09E-37	2.06E-22	2.27E-15	2.05E-11	5.98E-09	2.7E-07	4.01E-06	2.96E-05	~	0.26167	0.260785	0.259902	0.259023	0.258146	0.257272	0.2564	0.255531	0.254665	0.253802	0.252941
~	~	~	~	~	~	~	~	~	~	~	~	~	~	~	~	~	~	~	~	~	~	~
17.5	0	0	0	0	4.2E-251	4.1E-175	3.2E-129	2.2E-99	7.04E-79	3.45E-64	~	0.101004	0.100786	0.100568	0.10035	0.100131	0.099913	0.099695	0.099476	0.099258	0.09904	0.098822
18	0	0	0	0	1.7E-267	1.7E-186	1.4E-137	8.9E-105	6.1E-84	2.7E-68	~	0.095115	0.094917	0.094719	0.09452	0.094322	0.094123	0.093925	0.093726	0.093528	0.093329	0.093131
18.5	0	0	0	0	2.1E-284	3E-198	3.3E-146	2.2E-112	3.7E-89	1.63E-72	~	0.089418	0.089238	0.089059	0.08888	0.0887	0.08852	0.088341	0.088161	0.087981	0.087801	0.087621
19	0	0	0	0	7.3E-302	2.3E-210	4.1E-155	3.3E-119	1.5E-94	7.05E-77	~	0.083919	0.083758	0.083596	0.083435	0.083273	0.083111	0.082949	0.082787	0.082624	0.082462	0.082299
19.5	0	0	0	0	0	7.4E-223	2.7E-164	3.1E-126	4.2E-100	2.2E-81	~	0.078626	0.078481	0.078337	0.078192	0.078046	0.077901	0.077756	0.07761	0.077464	0.077318	0.077172
20	0	0	0	0	0	1E-235	9.5E-174	1.8E-133	8.1E-106	5.2E-86	~	0.073542	0.073413	0.073284	0.073154	0.073025	0.072895	0.072765	0.072635	0.072505	0.072374	0.072243

Figure B 3. Format of the output file (velocity field).

Appendix C. Instructions on Running the Standalone Maynord Model on a 32-bit Microsoft® Windows® 7 Computer

This application was compiled with the 32-bit version of the fully-licensed MATLAB® Compiler. You must run the appropriate application on a computer running 32-bit Microsoft® Windows® 7. It will not run on a 64-bit system.

The computer must be connected to the Internet in order to run the installation.

1. Copy the entire "prop_GUI2_win32" directory to your computer. It is recommended to copy it into your "Documents" directory.
2. Go into the "prop_GUI2_win32\Installer_win32" directory.
3. Run "MyAppInstaller_web.exe". This file will install the MATLAB® Compiler Runtime (MCR) on your computer and allow it to run standalone applications. The computer must be connected to the Internet as the installer needs to download additional files. The size of these downloaded files may be up to 639 Mb. Keep this in mind if your hard drive space is limited.
4. A Windows® message box saying, "Do you want the following application from an unknown publisher to make changes to this computer?" might pop up. Click "Yes".
5. Please wait while the installer prepares the necessary files. The installer will attempt to download files from the Internet. If your computer does not have a working Internet connection, then this step will fail.
6. The prop_GUI2_win32 1.0 window pops up. Click "Next->".
7. Choose the location of the installation directory. The default location is "C:\Program Files\prop_GUI2_win32". Click "Next->".
8. A message saying, "The destination folder "C:\Program Files\prop_GUI2_win32 does not exist. Create it?" might pop up. If so, click "Yes".
9. Choose the location of the Matlab Compiler Runtime directory. The default location is "C:\Program Files\MATLAB\MATLAB Compiler Runtime". Click "Next->".
10. A message saying, "The destination folder "C:\Program Files\MATLAB\MATLAB Compiler Runtime does not exist. Create it?" might pop up. If so, click "Yes".
11. Accept the license agreement. Select "Yes" and click "Next->".
12. In the Confirmation window, click "Install". Wait for the installation to complete.
13. Go into the "prop_GUI2_win32" directory and run "prop_GUI2_win32.exe". A splash screen will appear while the application is loading.

Instructions on data export

1. Run "prop_GUI2_win32.exe" from inside the "prop_GUI2_win32" directory. Enter the desired User-Defined Parameters.

2. Click “Calculate” in the Command Panel. The contour plots on the bottom and right hand side will populate.

3. If the plots are satisfactory, then click either the “Excel” or “ASCII” button to export the data in the desired format. Please wait until one data export process is complete before starting another. Make sure to click “Calculate” after any user-defined parameters are changed to ensure that the data is updated before it is exported. Clicking the “Reset” button will reset the User-Defined Parameters to the default values.

   a. The ASCII export option will create three comma-delimited text files named, “prop_velocity.txt”, “prop_shear.txt”, and “prop_erosion.txt” in the same folder as “prop_GUI2_win32.exe” resides. These text files can be imported into Microsoft® Excel®. Make sure to select comma as the delimiter while importing into Excel®.

   b. The Excel export option will generate an Excel® file named “prop_data_xx.xlsx”(*where, xx=current date and time stamp)*. This Excel® file will contain three sheets named Sheet1, Sheet2, and Sheet3. It will reside in the same directory as “prop_GUI2_win32.exe”. The three sheets contain the velocity, shear stress, and erosion rate data.

      Please be patient. The Excel data export can take up to 5 minutes. Please refrain from executing any other commands in the PropGUI window during this time. A message box will pop up to notify you when the export is complete.

Note: Microsoft® Excel® 2007 or a later version is required for the Excel® data export. Earlier versions do not support more than 256 columns of data; this application exports over 600 columns of data. Using earlier versions Excel® may cause this step to fail, or the data export to be incomplete.

The Excel® data file may be renamed after the export is complete. However, it must be saved with an “.xlsx” extension in order to support more than 256 columns. Do not save as an “.xls”.

Exporting data directly into Excel® requires a considerable amount of time. It is much faster, and more practical, to export the data as ASCII files and open them in Excel®.

Within the “prop_dataxx.xlsx” file, Sheet 1 contains the velocity data, Sheet 2 contains the shear stress data, and Sheet 3 contains the volumetric erosion rate data. The cells in the first column of each sheet, Range A4:A84, contain the y (lateral distance from centerline) values; the cells in the third row, Range B3:WC3, contain the x(distance behind propeller) values. The units of x and y are meters. Cell Range B4:WC84 contains the calculated data (velocity, shear stress, or erosion rate). The units are as follows: velocity – m/s, shear stress – Pascal, erosion rate – grams/(m^2 *s).

Appendix D. Instructions on Running the Standalone Maynord Model on a 64-bit Microsoft® Windows® 7 Computer

This application was compiled with the 64-bit version of the fully-licensed MATLAB® Compiler. You must run the appropriate application on a computer running 64-bit Microsoft® Windows® 7. It will not run on a 32-bit system.

The computer must be connected to the Internet in order to run the installation.

1. Copy the entire "prop_GUI2_win64" directory to your computer. It is recommended to copy it into your "Documents" directory.
2. Go into the "prop_GUI2_win64\Installer_win64" directory.
3. Run "MyAppInstaller_web.exe". This file will install the MATLAB® Compiler Runtime (MCR) on your computer and allow it to run standalone applications. The computer must be connected to the Internet as the installer needs to download additional files. The size of these downloaded files may be up to 701 Mb. Keep this in mind if your hard drive space is limited.
4. A Windows® message box saying, "Do you want the following application from an unknown publisher to make changes to this computer?" might pop up. Click "Yes".
5. Please wait while the installer prepares the necessary files. The installer will attempt to download files from the Internet. If your computer does not have a working Internet connection, then this step will fail.
6. The prop_GUI2_win64 1.0 window pops up. Click "Next->".
7. Choose the location of the installation directory. The default location is "C:\Program Files\prop_GUI2_win64". Click "Next->".
8. A message saying, "The destination folder "C:\Program Files\prop_GUI2_win64 does not exist. Create it?" might pop up. If so, click "Yes".
9. Choose the location of the Matlab Compiler Runtime directory. The default location is "C:\Program Files\MATLAB\MATLAB Compiler Runtime". Click "Next->".
10. A message saying, "The destination folder "C:\Program Files\MATLAB\MATLAB Compiler Runtime does not exist. Create it?" might pop up. If so, click "Yes".
11. Accept the license agreement. Select "Yes" and click "Next->".
12. In the Confirmation window, click "Install". Wait for the installation to complete.
13. Go into the "prop_GUI2_win64" directory and run "prop_GUI2_win64.exe". A splash screen will appear while the application is loading.

Instructions on data export

1. Run "prop_GUI2_win64.exe" from inside the "prop_GUI2_win64" directory. Enter the desired User-Defined Parameters.

2. Click “Calculate” in the Command Panel. The contour plots on the bottom and right hand side will populate.

3. If the plots are satisfactory, then click either the “Excel” or “ASCII” button to export the data in the desired format. Please wait until one data export process is complete before starting another. Make sure to click “Calculate” after any user-defined parameters are changed to ensure that the data is updated before it is exported. Clicking the “Reset” button will reset the User-Defined Parameters to the default values.

    a. The ASCII export option will create three comma-delimited text files named, “prop_velocity.txt”, “prop_shear.txt”, and “prop_erosion.txt” in the same folder as “prop_GUI2_win64.exe” resides. These text files can be imported into Microsoft® Excel®. Make sure to select comma as the delimiter while importing into Excel®.

    b. The Excel export option will generate an Excel® file named “prop_data_xx.xlsx”(*where, xx=current date and time stamp)*. This Excel® file will contain three sheets named Sheet1, Sheet2, and Sheet3. It will reside in the same directory as “prop_GUI2_win64.exe”. The three sheets contain the velocity, shear stress, and erosion rate data.

    Please be patient. The Excel data export can take up to 5 minutes. Please refrain from executing any other commands in the PropGUI window during this time. A message box will pop up to notify you when the export is complete.

Note: Microsoft® Excel® 2007 or a later version is required for the Excel® data export. Earlier versions do not support more than 256 columns of data; this application exports over 600 columns of data. Using earlier versions Excel® may cause this step to fail, or the data export to be incomplete.

The Excel® data file may be renamed after the export is complete. However, it must be saved with an “.xlsx” extension in order to support more than 256 columns. Do not save as an “.xls”.

Exporting data directly into Excel® requires a considerable amount of time. It is much faster, and more practical, to export the data as ASCII files and open them in Excel®.

Within the “prop_dataxx.xlsx” file, Sheet 1 contains the velocity data, Sheet 2 contains the shear stress data, and Sheet 3 contains the volumetric erosion rate data. The cells in the first column of each sheet, Range A4:A84, contain the y (lateral distance from centerline) values; the cells in the third row, Range B3:WC3, contain the x(distance behind propeller) values. The units of x and y are meters. Cell Range B4:WC84 contains the calculated data (velocity, shear stress, or erosion rate). The units are as follows: velocity – m/s, shear stress – Pascal, erosion rate – grams/(m^2 *s).